
Power up! Robust Graph Convolutional Network against Evasion Attacks based on Graph Powering

Ming Jin

University of California, Berkeley
jinming@berkeley.edu

Heng Chang

Tsinghua University
changh17@mails.tsinghua.edu.cn

Wenwu Zhu

Tsinghua University
wzhu@tsinghua.edu.cn

Somayeh Sojoudi

University of California, Berkeley
sojoudi@berkeley.edu

Abstract

Graph convolutional networks (GCNs) are powerful tools for graph-structured data. However, they have been recently shown to be prone to topological attacks. Despite substantial efforts to search for new architectures, it still remains a challenge to improve performance in both benign and adversarial situations *simultaneously*. In this paper, we re-examine the *fundamental building block* of GCN—the Laplacian operator—and highlight some basic flaws in the spatial and spectral domains. As an alternative, we propose an operator based on graph powering, and prove that it enjoys a desirable property of “spectral separation.” Based on the operator, we propose a robust learning paradigm, where the network is trained on a family of “smoothed” graphs that span a spatial and spectral range for generalizability. We also use the new operator in replacement of the classical Laplacian to construct an architecture with improved spectral robustness, expressivity and interpretability. The enhanced performance and robustness are demonstrated in extensive experiments.

1 Introduction

Graph convolutional networks (GCNs) [34] are powerful extensions of Convolutional Neural Networks (CNNs) to graph-structured data. Recently, GCNs and variants have been applied to a wide range of domains, achieving state-of-the-art performances in social networks [34], traffic prediction [46], recommendation systems [55], applied chemistry and biology [32, 21], computer vision [23, 50], and natural language processing [5, 26, 7, 41], just to name a few [56, 53].

GCNs belong to a family of *spectral methods* that deal with spectral representations of graphs. A fundamental ingredient of GCNs is the *graph convolution operation*, defined using the eigendecomposition of the graph Laplacian in the Fourier domain:

$$\mathbf{g}_\theta \star \mathbf{x} := \mathbf{U} \mathbf{g}_\theta(\mathbf{\Lambda}) \mathbf{U}^\top \mathbf{x}, \quad (1)$$

where $\mathbf{x} \in \mathbb{R}^n$ is the graph signal on the set of vertices \mathcal{V} , \mathbf{U} and $\mathbf{\Lambda}$ are the eigenvectors and eigenspectrum of $\mathbf{L} := \mathbf{D} - \mathbf{A}$ (where \mathbf{D} and \mathbf{A} are the degree matrix and the adjacency matrix, respectively), and \mathbf{g}_θ is a spectral function applied to the eigenspectrum. Because this operation is computational intensive for large graphs and non-spatially localized [11], early attempts relied on a parameterization with smooth coefficients [28] or a truncated expansion in terms of Chebyshev polynomials [27]. A milestone was set by [34], which pushed the state-of-the-art performance of semi-supervised learning using a vanilla GCN architecture that is based on a first-order approximation

of the Chebyshev polynomials. The network has the following layer-wise update rule:

$$\mathbf{H}^{(l+1)} := \sigma \left(\mathcal{A} \mathbf{H}^{(l)} \mathbf{W}^{(l)} \right), \quad (2)$$

where $\mathbf{H}^{(l)}$ is the l -th layer hidden state (with $\mathbf{H}^{(1)} := \mathbf{X}$ as nodal features), $\mathbf{W}^{(l)}$ is the l -th layer weight matrix, σ is the usual point-wise activation function, and \mathcal{A} is the convolution operator chosen to be the degree weighted Laplacian with some slight modifications [34]. Subsequent GCN variants have different architectures, but they all share the use of the Laplacian matrix as the convolution operator [56, 53].

1.1 Why not Laplacian?

Undoubtedly, the Laplacian operator (and its variants, e.g., normalized/powered Laplacian) plays a central role in spectral theory, and is a natural choice for a variety of algorithms such as principal component analysis, clustering and linear embeddings [14, 8]. *So what can be problematic with it?*

From a spatial perspective, GCNs with L layers cannot acquire nodal information beyond its L -distance neighbors (a fact to be verified); hence, it severely limits its scope of data fusion.

From a spectral perspective, one could demand better *spectral properties*, given that GCN is fundamentally a particular (yet effective) approximation of the spectral convolution (1). A key desirable property for generic spectral methods is known as ‘‘spectral separation,’’ namely the spectrum should comprise a few dominant eigenvalues whose associated eigenvectors reveal the sought structure in the graph. A well-known prototype is the Ramanujan property, for which the second leading eigenvalue of a d -regular graph is no larger than $2\sqrt{d-1}$, which is also enjoyed asymptotically by random d -regular graphs [22] and Erdős-Rényi graphs that are not too sparse [20].

In a more realistic scenario, consider the stochastic block model (SBM), which attempts to capture the essence of many networks, including social graphs, citation graphs, and even brain networks [29].

Definition 1 (Simplified stochastic block model). The graph \mathcal{G} with n nodes is drawn under $\text{SBM}(n, k, a_{\text{intra}}, a_{\text{inter}})$ if the nodes are evenly and randomly partitioned into k communities, and nodes i and j are connected with probability $a_{\text{intra}}/n \in [0, 1]$ if they belong to the same community, and $a_{\text{inter}}/n \in [0, 1]$ if they are from different communities.

It turns out that for community detection, the top k leading eigenvectors of the adjacency matrix \mathbf{A} play an important role. In particular, for the case of 2 communities, spectral bisection algorithms simply take the second eigenvector to reveal the community structure. This can be also seen from the expected adjacency matrix $\mathbb{E}[\mathbf{A}]$ under $\text{SBM}(n, 2, a_{\text{intra}}, a_{\text{inter}})$, which is a rank-2 matrix with the top eigenvalue $\frac{1}{2}(a_{\text{intra}} + a_{\text{inter}})$ and eigenvector $\mathbf{1}$, and the second eigenvalue $\frac{1}{2}(a_{\text{intra}} - a_{\text{inter}})$ and eigenvector $\boldsymbol{\sigma}$ such that $\sigma_i = 1$ if i is in community 1 and $\sigma_i = -1$ otherwise. More generally, the second eigenvalue is of particular theoretical interests because it controls at the first order how fast heat diffuses through graph, as depicted by the discrete Cheeger inequality [36].

While one would expect taking the second eigenvector of adjacency matrix suffices, it often fails in practice (even when it is theoretically possible to recover the clusters given the signal-to-noise ratio). This is especially true for sparse networks, whose average nodal degrees is a constant that does not grow with the network size. This is because the spectrum of the Laplacian or adjacency matrix is blurred by ‘‘outlier’’ eigenvalues in the sparse regime, which is often caused by high degree nodes [31]. Unsurprisingly, powering the Laplacian would be of no avail, because it does not change the eigenvectors or the ordering of eigenvalues. In fact, those outliers can become more salient after powering, thereby weakening the useful spectral signal even further.

Besides, pruning the largest degree nodes in the adjacency matrix or normalizing the Laplacian cannot solve the issue. To date, the best results for pruning does not apply down to the theoretical recovery threshold [15, 43, 35]; either outliers would persist or one could prune too much that the graph is destroyed. As for normalized Laplacian, it may overcorrect the large degree nodes, such that the leading eigenvectors would catch the ‘‘tails’’ of the graph, i.e., components weakly connected to the main graph.

In summary, Laplacian may not be the ideal choice due to its limited spatial scope of information fusion, and its undesirable artefacts in the spectral domain.

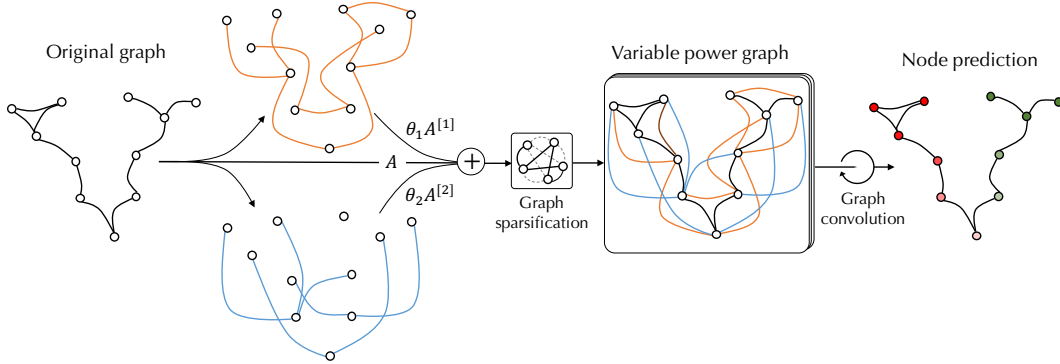


Figure 1: From the original graph, we first generate a family of distance graphs, which are weighted by parameters that gauge the influence strengths, (optionally) sparsified, and eventually combined to form a variable power graph. It can be used to construct a convolution operator or robust regularizer.

1.2 If not Laplacian, then what?

In searching for alternatives, potential choices are many, so it is necessary to clarify the goals. In view of the aforementioned pitfalls of Laplacian, one would naturally ask the question:

Can we find an operator that has wider spatial scope, more robust spectral properties, and is meanwhile interpretable and can even increase the expressive power of GCN?

From a perspective of *graph data analytics*, this question gauges how information is propagated and fused on a graph, and how we should interpret “adjacency” in a much broader sense. An image can be viewed as a regular grid, yet the operation of a CNN filter goes beyond the nearest pixel to a local neighborhood to extract useful features. What can be the analogous operation to an irregular graph?

From a perspective of *robust learning*, this question sheds light on the basic observation that real-world graphs are often noisy and even adversarial. The nice spectral properties of a graph topology can be lost with the presence of absence of edges. What are some principled ways to robustify the convolution operator and/or graph embeddings?

In this paper, we propose a *new* operator that aims at achieving this goal, as illustrated in Figure 1.

Definition 2 (Variable power operator). Consider an unweighted and undirected graph \mathcal{G} . Let $\mathbf{A}^{[k]}$ denote the k -distance adjacency matrix, i.e., $[\mathbf{A}^{[k]}]_{ij} = 1$ if and only if the shortest distance between nodes i and j is k . The variable power operator of order r is defined as:

$$\mathbf{A}_{\boldsymbol{\theta}}^{(r)} = \sum_{k=0}^r \theta_k \mathbf{A}^{[k]}, \quad (3)$$

where $\boldsymbol{\theta} := (\theta_0, \dots, \theta_r)$ is a set of parameters.

Clearly, $\mathbf{A}_{\boldsymbol{\theta}}^{(r)}$ is a natural extension of the classical adjacency matrix (i.e., $r = 1$ and $\theta_0 = \theta_1 = 1$). With power order $r > 1$, one can increase the spatial scope of information fusion on the graph when applying the convolution operation. It is also *interpretable*—the magnitude and the sign of θ_k can be viewed as “global influence strength” and “global influence propensity” at distance k , respectively.

Furthermore, we provide some theoretical justification of the proposed operator by establishing the following asymptotic property of spectral separation under the important SBM setting, which is, nevertheless, not enjoyed by the classical Laplacian operator or its normalized or powered versions. (All proofs are given in the supplementary material.)

Theorem 3 (Asymptotic spectral separation of variable power operator). Consider a graph \mathcal{G} drawn from $\text{SBM}(n, 2, a_{\text{intra}}, a_{\text{inter}})$. Assume that the signal-to-noise ratio $\xi_2^2/\xi_1 > 1$, where $\xi_1 = \frac{1}{2}(a_{\text{intra}} + a_{\text{inter}})$ and $\xi_2 = \frac{1}{2}(a_{\text{intra}} - a_{\text{inter}})$ (c.f., [18]). Suppose r is on the order of $c \log(n)$ for a constant c , such that $c \log(\xi_1) < 1/4$. Given nonvanishing θ_k for $k > r/2$, the variable power operator $\mathbf{A}_{\boldsymbol{\theta}}^{(r)}$ has the following spectral properties: (i) the leading eigenvalue is on the order of $\Theta(\|\boldsymbol{\theta}\|_1 \xi_1^r)$, the second leading eigenvalue is on the order of $\Theta(\|\boldsymbol{\theta}\|_1 \xi_2^r)$, and the rest are bounded

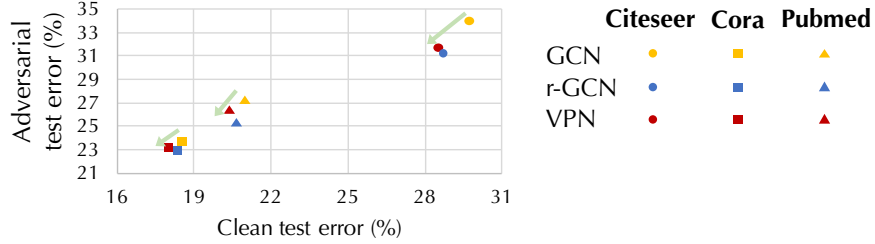


Figure 2: Our proposed framework can reduce test errors in both the clean dataset and the adversarial (10% attack rate) situation for all semi-supervised learning datasets (Citeseer, Cora, and Pubmed).

by $\|\theta\|_1 n^\epsilon \xi_1^{r/2} O(\log(n))$ for any fixed $\epsilon > 0$; and (ii) the two leading eigenvectors are sufficient to recover the two communities asymptotically (i.e., as n goes to infinity).

Intuitively, the above theoretical result suggests that the variable power operator is able to “magnify” *benign signals* from the latent graph structure while “suppressing” *noises* due to random artefacts. This is expected to improve spectral methods in general, especially when the benign signals tend to be overwhelmed by noises. Of course, real-world networks are more complex than SBM (albeit a good model). So for the rest of the paper, we will apply this insight to propose a robust graph learning paradigm in Section 2, as well as a new GCN architecture in Section 3. We also provide empirical evidence of the gain from this more favorable spectral behavior in Section 4. We believe our work is one of the first attempts to robustify GCN. Since the search for potential robust convolutional operators opens up ample opportunities, we will conclude in Section 5 with some future directions.

1.3 Related work

Beyond nearest neighbors. One limitation of using Laplacian in GCN is that the first layer only “sees” features of adjacent nodes. Several works have been proposed to address this issue [37, 2, 3]. For instance, adjacency matrix and its powered versions are used in [37, 2, 3] to construct GCN layers. However, simply powering the adjacency does not extract spectral gap and may even make the eigenspectrum more sensitive to perturbations. The architecture in [3] also introduced additional weight matrices for neighbors at different distances. But this could substantially increase the risk of overfitting in the low-data regime and make the network vulnerable to adversarial attacks.

Robust spectral theory. The robustness of spectral methods has been extensively studied for graph partitioning/clustering using adversarial perturbations or noise perturbations [38, 6, 19]. A common approach is to use regularization on the Laplacian [12, 4, 30]. Most recently, operators based on self-avoiding or nonbacktracking walks have become popular for SBM [42, 44, 10], which have been proved to achieve the theoretical detection threshold conjectured in [18]. Our work is partly motivated by the graph powering approach [1], which leveraged the result of [42, 10] to show a spectral gap of the powering operator. The main difference with this line of work is that these operators are studied only for spectral clustering algorithms, which does not incorporate nodal features. Our proposed variable power operator can be viewed as a kernel version of the graph powering operator [1], thus substantially increasing the capability of learning complex nodal interactions while maintaining the nice spectral property.

Robust graph neural network. While there is a surge of adversarial attacks on graph neural networks, very few methods have been proposed to defend against such attacks [47]. Existing works experimented adversarial training, namely to add or drop edges during training [16, 13]. “Soft labels” have also been employed [13]. However, the main issue is that these methods are direct applications of known methods from computer vision [49, 25, 48], and do not exploit the unique characteristics of graph-structured data. In particular, it has not been shown whether such approach will reduce performance in the usual testing with clean data, but it is likely to be a collateral cost of such training techniques. By comparison, our work shows that it is indeed possible to simultaneously improve both performance on clean data and robustness against adversarial attacks, as shown in Figure 2 (details are presented in Section 4).

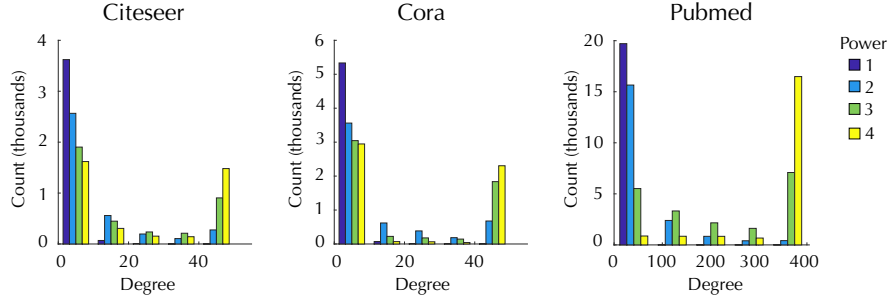


Figure 3: Degree distribution in the original graph and the powered graphs for 3 datasets (Table 1). Nodes with degrees more than 50 (400) are assigned to the largest bin for Citeseer and Cora (Pubmed).

2 Robust training based on graph powering

Given a graph \mathcal{G} , consider a family of its powered graphs, $\{\mathcal{G}^{(2)}, \dots, \mathcal{G}^{(r)}\}$, where $\mathcal{G}^{(k)}$ is obtained by connecting nodes with distance less than or equal to k . This can be regarded as “graph smoothing”, because as k increases, the graph appears more homogenized (as shown in Figure 3). In particular, it can help near-isolated nodes (i.e., low-degree vertices), since they become connected beyond their nearest neighbors. By comparison, simply raising the adjacency matrix to its r -th power will make them appear even *more isolated*, because it inadvertently promotes nodes with high degrees or nearby loops much more substantially as a result of feedback.

At a higher level, graph smoothing is close to data augmentation—from a given graph, we generate a sequence of graphs that are similar in the spatial domain. Furthermore, the powered graphs can extract spectral gaps in the original graph that despite local irregularities, thus boosting the signal-to-noise ratio in the spectral domain.

In the following, we propose the first application of graph powering, namely to regularize GCN training. Consider a generic learning task on a graph \mathcal{G} with data \mathcal{D} . The loss function is denoted by $\ell(\mathcal{W}; \mathcal{G}, \mathcal{D})$ for a particular GCN architecture parametrized by \mathcal{W} . For instance, in semi-supervised learning, \mathcal{D} consists of features and labels on a small set of nodes (see Table 1), and ℓ is the cross-entropy loss over all labeled examples [34]. Instead of minimizing over $\ell(\mathcal{W}; \mathcal{G}, \mathcal{D})$ alone, we propose the following regularized objective:

$$\ell(\mathcal{W}; \mathcal{G}, \mathcal{D}) + \sum_{k=2}^r \alpha_k \ell(\mathcal{W}; \mathcal{G}^{(k)}, \mathcal{D}), \quad (\text{r-GCN})$$

where $\alpha_k \geq 0$ gauges how much information one desires to “distill” from powered graph $\mathcal{G}^{(k)}$ into the learning process.

By minimizing the (r-GCN) objective, one seeks to optimize the network parameter \mathcal{W} on multiple graphs simultaneously, which collectively comprise a wider spectrum of spatial and spectral variations. This is beneficial in two ways: **(i)** in the *low-data regime*, like semi-supervised learning, it helps to reduce the variance to improve generalization; **(ii)** in the *adversarial setting*, it robustifies the network since it is more likely that the perturbed network is contained in the wider spectrum during training.

3 New architecture: variable power network

In this section, we propose another application of the variable power operator, namely to construct a new GCN architecture. By using the variable power operator illustrated in Figure 1, this network can have broader scope of spatial fusion, more expressive power, and enhanced spectral robustness. But as the power grows, the network eventually becomes dense, as shown in Figure 3. To manage this increased complexity and make the network more robust against adversarial attacks, we propose a new pruning mechanism.

Graph sparsification. Given a graph $\mathcal{G} := (\mathcal{V}, \mathcal{E}^{[1]})$, consider its powered version $\mathcal{G}^{(r)} := (\mathcal{V}, \mathcal{E}^{(r)})$ and a sequence of intermediate graphs $\mathcal{G}^{[2]}, \dots, \mathcal{G}^{[r]}$, where $\mathcal{G}^{[k]} := (\mathcal{V}, \mathcal{E}^{[k]})$ is constructed by

Table 1: Citation datasets. Label rate denotes the fraction of training labels in each dataset.

Dataset	Nodes	Edges	Features	Classes	Label rates
Citeseer	3,327	4,732	3,703	6	0.036
Cora	2,708	5,429	1,433	7	0.052
Pubmed	19,717	44,338	500	3	0.003

connecting two vertices if and only if the shortest distance is k in \mathcal{G} . Clearly, $\{\mathcal{E}^{[k]}\}_{k=1}^r$ forms a partition of $\mathcal{E}^{(r)}$. For each node $i \in \mathcal{V}$, denote its r -neighborhood by $\mathcal{N}_r(i) := \{j \in \mathcal{V} \mid d_{\mathcal{G}}(i, j) \leq r\}$, which is identical to the set of nodes adjacent to i in $\mathcal{G}^{[r]}$.

Next, for each edge within this neighborhood, we associate a value using some suitable distance metric ϕ to measure ‘‘aloofness.’’ For instance, it can be the usual Euclidean distance or correlation distance in the feature space. Based on this formulation, we prune an edge $e := (i, j)$ in $\mathcal{E}^{(r)}$ if the value is larger than a threshold $\tau(i, j)$, and denote the edge set after pruning $\bar{\mathcal{E}}^{(r)}$. Then, we can construct a new sequence of sparsified graphs, $\bar{\mathcal{G}}^{[k]}$ with edge sets $\bar{\mathcal{E}}^{[k]} = \mathcal{E}^{[k]} \cap \bar{\mathcal{E}}^{(r)}$ and adjacency matrix $\bar{\mathbf{A}}^{[k]}$. Hence, the variable power operator is given by

$$\bar{\mathbf{A}}_{\theta}^{(r)} = \sum_{k=0}^r \theta_k \bar{\mathbf{A}}^{[k]} \quad (4)$$

Due to the influence of high-degree nodes in the spectral domain, one can *adaptively* choose the thresholds $\tau(i, j)$ to mitigate their effects. Specifically, we choose τ to be a small number if either i or j are nodes with high degrees, thereby making the sparsification more influential in densely connected neighborhoods than weakly connected parts.

Layer-wise update rule. To demonstrate the effectiveness of the proposed operator, we adopt the vanilla GCN strategy (2). Importantly, we replace the graph convolutional operator \mathcal{A} with the variable power operator. In particular,

$$\mathcal{A} = \mathbf{D}^{-\frac{1}{2}} (\mathbf{I} + \bar{\mathbf{A}}_{\theta}^{(r)}) \mathbf{D}^{-\frac{1}{2}}, \quad (\text{VPN})$$

where $D_{ii} = 1 + |\{j \in \mathcal{V} \mid d_{\mathcal{G}}(i, j) = 1\}|$. The introduction of \mathbf{I} is reminiscent of the ‘‘renormalization trick’’ [34], but it can be also viewed as a regularization strategy in this context, which is well-known to improve the spectral robustness [4, 30]. We show that this construction, called variable power network (VPN), immediately increases the scope of data fusion by a factor of r .

Theorem 4. By choosing \mathcal{A} with (VPN) in the layer-wise update rule (2), the output at each node from a L -layer GCN depends on neighbors within $L * r$ edges.

Since we proved that the variable power operator has nice spectral separation in Theorem 3, VPN is expected to promote useful spectral signals from the graph topology. This claim is substantiated with the following proposition.

Proposition 5. Given a graph with two hidden communities. Consider a 2-layer GCN architecture with layer-wise update rule (2). Suppose that \mathcal{A} has a spectral gap. Further, assume that the leading two eigenvectors are asymptotically aligned with $\mathbf{1}$ and $\boldsymbol{\nu}$, i.e., the community membership vector, and that both are in the range of feature matrix \mathbf{X} . Then, there exists a configuration of $\mathbf{W}^{(1)}$ and $\mathbf{W}^{(2)}$ such that the GCN outputs can recover the community with high probability.

This result further justifies the rationale of the (VPN) architecture.

4 Experiments

4.1 Semi-supervised node classification

Experimental setup. We followed closely the setup of [54, 34], where three citation networks are tested, namely Citeseer, Cora and Pubmed, whose nodes are documents and edges are citation links (see Table 1 for more details). We used the same dataset splits as in [54, 34] with 20 labels per class for training, 500 labeled samples for hyperparameter setting, and 1,000 samples for testing.

Table 2: Experimental results (in percent) on node classification citation networks [54].

Model	Citeseer	Cora	Pubmed
ManiReg [9]	60.1	59.5	70.7
SemiEmb [51]	59.6	59.0	71.1
LP [57]	45.3	68.0	63.0
DeepWalk [45]	43.2	67.2	65.3
ICA [39]	69.1	75.1	73.9
Planetoid [54]	64.7	75.7	77.2
Vanilla GCN [34]	70.3	81.5	79.0
r-GCN (this paper)	71.3±0.54	81.7±0.23	79.3±0.31
VPN (this paper)	71.4±0.57	81.9±0.32	79.6±0.39

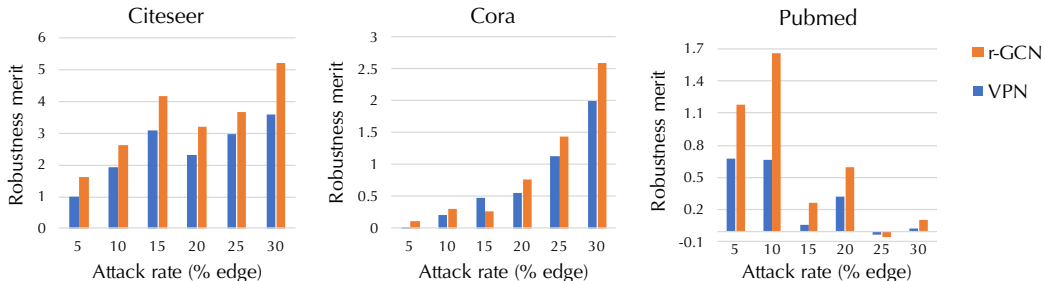


Figure 4: Robustnes merit $\left(\text{accuracy}_{\text{proposed-method}}^{\text{post-attack}} - \text{accuracy}_{\text{vanilla GCN}}^{\text{post-attack}} \right)$ reported in percentage.

To facilitate comparison, we use the same hyperparameters as vanilla GCN [34], including number of layers (2), number of hidden units (16), dropout rates (0.5), weight decay ($5e-4$), and weight initialization [24] implemented in Tensorflow. We chose a fixed number of training epochs (200) for all experiments. We note that the citation datasets are extremely sensitive to initializations; as such, we report the test accuracy for the top 50 runs out of 100 random initializations sorted by the *validation* accuracy. We used Adam [33] with a learning rate of 0.01 except for θ (VPN), which was chosen to be $1e-5$ to stabilize training.

Graph powering can influence degree distributions, as is shown in Figure 3. The effect is more salient for Pubmed than Citeseer and Cora, due to the prevalence of high degree nodes. Hence, we chose the power order to be 4 for r-GCN on Citeseer and Cora, and 3 for Pubmed, and reduced the order by 1 for VPN. We set α_k to be 0.5 for the corresponding power order and 0 otherwise in r-GCN. To enhance robustness against evasion attack, we adaptively chose the threshold of graph sparsification such that the size of the powered neighborhood of each node doubles the size of its original adjacent neighborhood. As a side remark, one can easily obtain $\mathbf{A}^{(r)}$ with $\mathbb{1}[(\mathbf{I} + \mathbf{A})^r > 0]$, and recursively calculate $\mathbf{A}^{[k]}$. The proposed methods have similar computational complexity as vanilla GCN as a result of sparsification.

Performance. Results are summarized in Table 2. By replacing Laplacian with our new operator, we see an immediate improvement of performance. This numerically substantiates the claim made in Section 1, that an operator with better spectral properties are expected to behave stronger, since it can boost useful graph information and learn an effective embedding from limited data. We also see that a succinct parametrization of the global influence relation in VPN is able to increase the expressivity of the network. For instance, the learned θ at distances 2 and 3 for Citeseer are $3.15e-3$ and $3.11e-3$ with p -value less than $1e-5$. This implies that the network tends to put more trust in closer neighbors. Further evidences are shown in the supplementary material, where we visualize the learned embeddings using t-SNE [40].

4.2 Defense against evasion attacks

To evaluate the robustness of the learned network, we considered the setting of evasion attacks, where an adversary can freely add or drop edges between any nodes. For the attack method, we used DICE

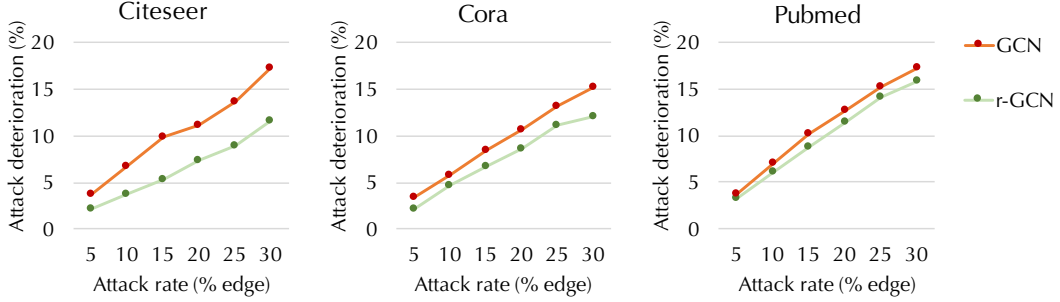


Figure 5: Attack deterioration $\left(1 - \text{accuracy}_{\mathcal{V}^{\text{attacked}}}^{\text{post-attack}} / \text{accuracy}_{\mathcal{V}^{\text{attacked}}}^{\text{pre-attack}}\right)$ reported in percentage.

[58], because it is a simple yet strong global attack with an interpretable strategy (remove internally, insert externally). In particular, it randomly disconnects nodes from the same class and connects nodes from different classes. We further modulated the severity by varying the attack rate, which corresponds to the percentage of edges to be attacked. All the networks are identically constructed and trained as the previous section.

Evaluation metrics. In addition to the post-attack accuracy, we propose two new metrics, namely “robustness merit” and “attack deterioration.” The former is the difference between the post-attack accuracy of the vanilla GCN and the proposed method. The latter is motivated by Theorem 4. It recognizes the fact that due to the limited spatial scope of GCN, any added/dropped edges can only affect nodes within the spatial scope in the original network. By delineating this set of “theoretically affected” nodes, $\mathcal{V}^{\text{attacked}}$, one can then evaluate the attack effect on the model prediction, i.e., $1 - \text{accuracy}_{\mathcal{V}^{\text{attacked}}}^{\text{post-attack}} / \text{accuracy}_{\mathcal{V}^{\text{attacked}}}^{\text{pre-attack}}$. This metric is particularly useful when the attack rate is small, such that $\mathcal{V}^{\text{attacked}}$ is very different from the test data points. But one should be cautious that it only makes sense to compare “attack deterioration” for networks with the same scope, because otherwise $\mathcal{V}^{\text{attacked}}$ might be quite different.

Robustness evaluation. Results for both metrics are shown in Figures 4 and 5. In general, both methods are able to substantially improve the defense against evasion attacks. The enhancement is more notable as the attack rate grows, implying that the learned embedding is robust to topological changes. This is in alignment with the spectral gap theory developed in Theorem 3, which also allows random connections between different communities without drastically changing the spectral behavior. It can be also observed that the proposed structures are more robust in Citeseer and Cora than Pubmed. In addition to the low label rates, we conjectured that topological attacks are more difficult to defend for networks with prevalent high-degree nodes, because the attacker can bring in more irrelevant vertices by simply adding an adversarial link to the high-degree nodes.

5 Conclusions

Graph convolutional network has become a powerful tool to solve challenging problems on graph-structured data. However, it has also been shown to be vulnerable to topological attacks. Despite the substantial efforts in searching for capable GCN architectures, one fundamental question remains: How to improve performance and *meanwhile* enhance robustness? Real-world networks are often noisy, uncertain, and even adversarial. A robust network is not only able to perform well on known datasets, but is also expected to generalize better in these adverse scenarios.

This paper challenges the fundamental building block of existing GCN architectures—the Laplacian operator. In particular, we highlighted two basic flaws of Laplacian, namely the limited scope of information fusion in the *spatial domain* and undesirable artefacts in the *spectral domain*. As an alternative, we proposed the variable power operator that is expected to alleviate the issues. We showed that it can be regarded as a kernel function that extracts spectral gaps that are buried under local irregularities, and it can increase the spatial scope by a factor of the power order.

Based on this new graph convolution operator, we first proposed a robust learning paradigm. The key idea is to use “graph smoothing” to construct a family of graphs that span a wide range in

the spatial and spectral domains. Incorporating them in the training objective allows information to be distilled from these powered graphs with nicer spectral properties. Furthermore, proposed a new GCN architecture using the variable power operator. It is a simple network, yet it inherits spectral robustness and is more expressive and interpretable—we can simultaneously learn the feature transformation function and the global influence parameters at different distances. Experimental evaluations on benchmarks showed notable improvement in the performance of semi-supervised learning *and* robustness against evasion attacks, further validating the efficacy of the framework.

Overall, as a spectral method, GCN can benefit from spectral robustness. Hence, it is promising to rethink the fundamental operator to use for graph convolution and explore various possibilities.

References

- [1] Emmanuel Abbe, Enric Boix, Peter Ralli, and Colin Sandon. Graph powering and spectral robustness. *arXiv preprint arXiv:1809.04818*, 2018.
- [2] Sami Abu-El-Haija, Amol Kapoor, Bryan Perozzi, and Joonseok Lee. N-GCN: Multi-scale graph convolution for semi-supervised node classification. *arXiv preprint arXiv:1802.08888*, 2018.
- [3] Sami Abu-El-Haija, Bryan Perozzi, Amol Kapoor, Hrayr Harutyunyan, Nazanin Alipourfard, Kristina Lerman, Greg Ver Steeg, and Aram Galstyan. Mixhop: Higher-order graph convolution architectures via sparsified neighborhood mixing. *arXiv preprint arXiv:1905.00067*, 2019.
- [4] Arash A Amini, Aiyu Chen, Peter J Bickel, Elizaveta Levina, et al. Pseudo-likelihood methods for community detection in large sparse networks. *The Annals of Statistics*, 41(4):2097–2122, 2013.
- [5] James Atwood and Don Towsley. Diffusion-convolutional neural networks. In *NIPS 2016*, pages 1993–2001, 2016.
- [6] Sivaraman Balakrishnan, Min Xu, Akshay Krishnamurthy, and Aarti Singh. Noise thresholds for spectral clustering. In *NIPS 2011*, pages 954–962, 2011.
- [7] Joost Bastings, Ivan Titov, Wilker Aziz, Diego Marcheggiani, and Khalil Sima’an. Graph convolutional encoders for syntax-aware neural machine translation. In *EMNLP 2017*, pages 1957–1967, 2017.
- [8] Mikhail Belkin and Partha Niyogi. Laplacian eigenmaps and spectral techniques for embedding and clustering. In *NIPS 2002*, pages 585–591, 2002.
- [9] Mikhail Belkin, Partha Niyogi, and Vikas Sindhwani. Manifold regularization: A geometric framework for learning from labeled and unlabeled examples. *Journal of Machine Learning Research*, 7:2399–2434, 2006.
- [10] Charles Bordenave, Marc Lelarge, and Laurent Massoulié. Non-backtracking spectrum of random graphs: community detection and non-regular ramanujan graphs. In *FOCS 2015*, pages 1347–1357. IEEE, 2015.
- [11] Joan Bruna, Wojciech Zaremba, Arthur Szlam, and Yann LeCun. Spectral networks and locally connected networks on graphs. In *ICLR 2014*, 2014.
- [12] Kamalika Chaudhuri, Fan Chung, and Alexander Tsiatas. Spectral clustering of graphs with general degrees in the extended planted partition model. *Journal of Machine Learning Research*, 2012:1–23.
- [13] Jinyin Chen, Yangyang Wu, Xiang Lin, and Qi Xuan. Can adversarial network attack be defended? *arXiv preprint arXiv:1903.05994*, 2019.
- [14] Fan RK Chung and Fan Chung Graham. *Spectral graph theory*. Number 92. American Mathematical Soc., 1997.
- [15] Amin Coja-Oghlan. Graph partitioning via adaptive spectral techniques. *Combinatorics, Probability and Computing*, 19(2):227–284, 2010.
- [16] Hanjun Dai, Hui Li, Tian Tian, Xin Huang, Lin Wang, Jun Zhu, and Le Song. Adversarial attack on graph structured data. In *ICML 2018*, pages 1123–1132, 2018.
- [17] Chandler Davis and William Morton Kahan. The rotation of eigenvectors by a perturbation: III. *SIAM Journal on Numerical Analysis*, 7(1):1–46, 1970.

- [18] Aurelien Decelle, Florent Krzakala, Cristopher Moore, and Lenka Zdeborová. Asymptotic analysis of the stochastic block model for modular networks and its algorithmic applications. *Physical Review E*, 84(6):066106, 2011.
- [19] Ilias Diakonikolas, Gautam Kamath, Daniel Kane, Jerry Li, Ankur Moitra, and Alistair Stewart. Robust estimators in high-dimensions without the computational intractability. *SIAM Journal on Computing*, 48(2):742–864, 2019.
- [20] Uriel Feige and Eran Ofek. Spectral techniques applied to sparse random graphs. *Random Structures & Algorithms*, 27(2):251–275, 2005.
- [21] Alex Fout, Jonathon Byrd, Basir Shariat, and Asa Ben-Hur. Protein interface prediction using graph convolutional networks. In *NIPS 2017*, pages 6530–6539, 2017.
- [22] Joel Friedman. A proof of alon’s second eigenvalue conjecture and related problems. *Mem. Amer. Math. Soc.*, (910), 2004.
- [23] Victor Garcia and Joan Bruna. Few-shot learning with graph neural networks. *arXiv preprint arXiv:1711.04043*, 2017.
- [24] Xavier Glorot and Yoshua Bengio. Understanding the difficulty of training deep feedforward neural networks. In *AISTATS 2010*, pages 249–256, 2010.
- [25] Ian J Goodfellow, Jonathon Shlens, and Christian Szegedy. Explaining and harnessing adversarial examples. In *ICLR 2015*, 2015.
- [26] Will Hamilton, Zhitao Ying, and Jure Leskovec. Inductive representation learning on large graphs. In *NIPS 2017*, pages 1024–1034, 2017.
- [27] David K Hammond, Pierre Vandergheynst, and Rémi Gribonval. Wavelets on graphs via spectral graph theory. *Applied and Computational Harmonic Analysis*, 30(2):129–150, 2011.
- [28] Mikael Henaff, Joan Bruna, and Yann LeCun. Deep convolutional networks on graph-structured data. *arXiv preprint arXiv:1506.05163*, 2015.
- [29] Paul W Holland, Kathryn Blackmond Laskey, and Samuel Leinhardt. Stochastic blockmodels: First steps. *Social Networks*, 5(2):109–137, 1983.
- [30] Antony Joseph, Bin Yu, et al. Impact of regularization on spectral clustering. *The Annals of Statistics*, 44(4):1765–1791, 2016.
- [31] Emilie Kaufmann, Thomas Bonald, and Marc Lelarge. A spectral algorithm with additive clustering for the recovery of overlapping communities in networks. In *ALT 2016*, pages 355–370. Springer, 2016.
- [32] Steven Kearnes, Kevin McCloskey, Marc Berndl, Vijay Pande, and Patrick Riley. Molecular graph convolutions: moving beyond fingerprints. *Journal of computer-aided molecular design*, 30(8):595–608, 2016.
- [33] Diederik P Kingma and Jimmy Ba. Adam: A method for stochastic optimization. In *ICLR 2015*, 2014.
- [34] Thomas N Kipf and Max Welling. Semi-supervised classification with graph convolutional networks. In *ICLR 2017*, 2017.
- [35] Can M Le, Elizaveta Levina, and Roman Vershynin. Sparse random graphs: regularization and concentration of the laplacian. *arXiv preprint arXiv:1502.03049*, 2015.
- [36] James R Lee, Shayan Oveis Gharan, and Luca Trevisan. Multiway spectral partitioning and higher-order cheeger inequalities. *Journal of the ACM*, 61(6):37, 2014.
- [37] John Boaz Lee, Ryan A Rossi, Xiangnan Kong, Sungchul Kim, Eunye Koh, and Anup Rao. Higher-order graph convolutional networks. *arXiv preprint arXiv:1809.07697*, 2018.
- [38] Zhenguo Li, Jianzhuang Liu, Shifeng Chen, and Xiaou Tang. Noise robust spectral clustering. In *ICCV 2007*, pages 1–8. IEEE, 2007.
- [39] Qing Lu and Lise Getoor. Link-based classification. In *ICML 2003*, pages 496–503, 2003.
- [40] Laurens van der Maaten and Geoffrey Hinton. Visualizing data using t-SNE. *Journal of machine learning research*, 9(Nov):2579–2605, 2008.
- [41] Diego Marcheggiani and Ivan Titov. Encoding sentences with graph convolutional networks for semantic role labeling. In *EMNLP 2017*, pages 1506–1515, 2017.

- [42] Laurent Massoulié. Community detection thresholds and the weak ramanujan property. In *STOC 2014*, pages 694–703. ACM, 2014.
- [43] Elchanan Mossel, Joe Neeman, and Allan Sly. Stochastic block models and reconstruction. *arXiv preprint arXiv:1202.1499*, 2012.
- [44] Elchanan Mossel, Joe Neeman, and Allan Sly. A proof of the block model threshold conjecture. *arXiv preprint arXiv:1311.4115*, 2013.
- [45] Bryan Perozzi, Rami Al-Rfou, and Steven Skiena. Deepwalk: online learning of social representations. In *KDD 2014*, pages 701–710, 2014.
- [46] Afshin Rahimi, Trevor Cohn, and Timothy Baldwin. Semi-supervised user geolocation via graph convolutional networks. In *ACL 2018*, volume 1, pages 2009–2019, 2018.
- [47] Lichao Sun, Ji Wang, Philip S Yu, and Bo Li. Adversarial attack and defense on graph data: A survey. *arXiv preprint arXiv:1812.10528*, 2018.
- [48] Christian Szegedy, Vincent Vanhoucke, Sergey Ioffe, Jon Shlens, and Zbigniew Wojna. Rethinking the inception architecture for computer vision. In *CVPR 2016*, pages 2818–2826, 2016.
- [49] Christian Szegedy, Wojciech Zaremba, Ilya Sutskever, Joan Bruna, Dumitru Erhan, Ian Goodfellow, and Rob Fergus. Intriguing properties of neural networks. In *ICLR 2014*, 2014.
- [50] Xiaolong Wang, Yufei Ye, and Abhinav Gupta. Zero-shot recognition via semantic embeddings and knowledge graphs. In *CVPR 2018*, pages 6857–6866, 2018.
- [51] Jason Weston, Frédéric Ratle, Hossein Mobahi, and Ronan Collobert. Deep learning via semi-supervised embedding. *Neural Networks: Tricks of the Trade (2nd ed.)*, pages 639–655, 2012.
- [52] Hermann Weyl. Das asymptotische verteilungsgesetz der eigenwerte linearer partieller differentialgleichungen (mit einer anwendung auf die theorie der hohlraumstrahlung). *Mathematische Annalen*, 71(4):441–479, 1912.
- [53] Zonghan Wu, Shirui Pan, Fengwen Chen, Guodong Long, Chengqi Zhang, and Philip S Yu. A comprehensive survey on graph neural networks. *arXiv preprint arXiv:1901.00596*, 2019.
- [54] Zhilin Yang, William W. Cohen, and Ruslan Salakhutdinov. Revisiting semi-supervised learning with graph embeddings. In *ICML 2016*, pages 40–48, 2016.
- [55] Rex Ying, Ruining He, Kaifeng Chen, Pong Eksombatchai, William L Hamilton, and Jure Leskovec. Graph convolutional neural networks for web-scale recommender systems. In *KDD 2018*, pages 974–983. ACM, 2018.
- [56] Jie Zhou, Ganqu Cui, Zhengyan Zhang, Cheng Yang, Zhiyuan Liu, and Maosong Sun. Graph neural networks: A review of methods and applications. *arXiv preprint arXiv:1812.08434*, 2018.
- [57] Xiaojin Zhu, Zoubin Ghahramani, and John D. Lafferty. Semi-supervised learning using gaussian fields and harmonic functions. In *ICML 2003*, pages 912–919, 2003.
- [58] Daniel Zügner and Stephan Günnemann. Adversarial attacks on graph neural networks via meta learning. In *ICLR 2019*, 2019.

A Proof of Theorem 4

To validate the claim, we prove a more general result. Consider a graph \mathcal{G} and its powered graph $\mathcal{G}^{(r)}$, whose adjacency matrices are \mathbf{A} and $\mathbf{A}^{(r)}$, respectively. Since the support of $\mathbf{A}_\theta^{(r)}$ is identical to that of $\mathbf{A}^{(r)}$, we will focus on $\mathbf{A}^{(r)}$ for notational simplicity. For any signal $\mathbf{f} : \mathcal{V} \mapsto \mathbb{R}^{|\mathcal{V}|}$ on a graph, denote the support of the signal f_v on node $v \in \mathcal{V}$ by \mathcal{S}_v^f , i.e., f_v only depends on the signals on nodes in \mathcal{S}_v^f . Then, it is easy to see that the signal $\mathbf{g} \triangleq \mathbf{A}\mathbf{f}$ has support $\mathcal{S}_v^g \subseteq \cup_{u \sim_r v} \mathcal{S}_u^f$, where $u \sim_r v$ denotes adjacency relation on $\mathcal{G}^{(r)}$ defined by $\mathbf{A}^{(r)}$. Clearly, the set defined by $\{u \in \mathcal{V} \mid u \sim_r v\}$ is identical to $\{u \in \mathcal{V} \mid d_{\mathcal{G}}(u, v) \leq r\}$, where $d_{\mathcal{G}}(u, v)$ denotes the shortest distance from u to v on \mathcal{G} .

Also, we see that element-wise operation does not expand the support, i.e., for any element-wise activation σ , the signal $\mathbf{g}_\sigma \triangleq \sigma(\mathbf{f})$ has support $\mathcal{S}_v^{g_\sigma} \subseteq \mathcal{S}_v^f$. In particular, we can prove the claim

by iteratively applying the function composition layer by layer, since each layer is of the form $\sigma(\mathbf{A}_\theta^{(r)} \mathbf{H}^{(l)} \mathbf{W}^{(l)})$, where $\mathbf{H}^{(l)}$ is the hidden state at layer l and $\mathbf{W}^{(l)}$ is the corresponding weight matrix. Hence after L iterations of layer-wise updates, the support of the output on v is given by $\{u \in \mathcal{V} \mid d_{\mathcal{G}}(u, v) \leq r * L\}$.

B Proof of Proposition 5

Let λ_1 and λ_2 be the two leading eigenvalues of $\bar{\mathbf{A}}$ with corresponding eigenvectors ϕ_1 and ϕ_2 , respectively. Without loss of generality, assume that both eigenvalues are nonnegative. Under the assumption that ϕ_1 and ϕ_2 lie in the range of \mathbf{X} , there exists a $\mathbf{W}^{(1)}$ such that $\mathbf{X}\mathbf{W}^{(1)} = [\phi_1 \ \phi_2]$. So the output of the first layer with ReLU activation is given by:

$$\mathbf{H}^{(1)} = \sigma(\bar{\mathbf{A}}\mathbf{X}\mathbf{W}^{(1)}) = \sigma(\bar{\mathbf{A}}[\phi_1 \ \phi_2]) \quad (5)$$

$$= [\lambda_1\sigma(\phi_1) \ \lambda_2\sigma(\phi_2)] \quad (6)$$

$$= [\lambda_1(\mathbf{1} + \sigma(\mathbf{h}_1)) \ \lambda_2(\frac{1}{2}\boldsymbol{\nu} + \frac{1}{2}\mathbf{1} + \sigma(\mathbf{h}_2))] \quad \text{where } \|\mathbf{h}_1\| = o(1) \text{ and } \|\mathbf{h}_2\| = o(1) \quad (7)$$

where (6) is due to the definition of eigenvectors and that σ is an element-wise operation, and (7) is due to the asymptotic alignment condition and the fact that $\sigma(\boldsymbol{\nu}) = \frac{1}{2}\boldsymbol{\nu} + \frac{1}{2}\mathbf{1}$. Therefore, by choosing

the last layer weight $\mathbf{W}^{(2)} = \begin{bmatrix} -\frac{1}{\lambda_1\lambda_2} & \frac{1}{\lambda_1\lambda_2} \\ \frac{1}{\lambda_2^2} & -\frac{1}{\lambda_2^2} \end{bmatrix}$, the output of the last layer is given by:

$$\begin{aligned} \mathbf{Y} &= \bar{\mathbf{A}}\mathbf{H}^{(1)}\mathbf{W}^{(2)} \\ &= \bar{\mathbf{A}}[\lambda_1(\mathbf{1} + \sigma(\mathbf{h}_1)) \ \lambda_2(\frac{1}{2}\boldsymbol{\nu} + \frac{1}{2}\mathbf{1} + \sigma(\mathbf{h}_2))] \mathbf{W}^{(2)} \\ &= [\lambda_1^2\mathbf{1} + \mathbf{h}'_1 \quad \frac{\lambda_2^2}{2}\boldsymbol{\nu} + \frac{\lambda_1\lambda_2}{2}\mathbf{1} + \mathbf{h}'_2] \mathbf{W}^{(2)} \\ &= [\boldsymbol{\nu} + \mathbf{h}''_1 \quad -\boldsymbol{\nu} + \mathbf{h}''_2] \end{aligned}$$

where $\|\mathbf{h}'_k\|_2 = o(1)$, $\|\mathbf{h}''_k\|_2 = o(1)$ for $k = 1, 2$. Therefore, after the softmax operation, we can see that the 2-layer output recovers the membership of the elements exactly.

One general remark is that while the above argument is not limited to the leading two eigenvalues/eigenvectors, from the form of $\mathbf{W}^{(2)}$ whose elements depend inversely on the corresponding eigenvalues, we can expect more numerical stability (and hence easier learning) when the corresponding eigenvalues are large.

C Proof of Theorem 3

Consider a stochastic block model with two communities, where the intra-community connection probability is a_{intra}/n and the inter-community connection probability is a_{inter}/n , and assume that $a_{\text{intra}} > a_{\text{inter}}$. Let $\xi_1 = \frac{a_{\text{intra}} + a_{\text{inter}}}{2}$ and $\xi_2 = \frac{a_{\text{intra}} - a_{\text{inter}}}{2}$, which correspond to the first and second eigenvalues of the expected adjacency matrix of the above model. Let $\boldsymbol{\nu}$ denote the community label vector, with $\nu_i = \pm 1$ depending on the membership of node i . For weak recovery, we assume the detectability condition [18]:

$$\xi_2^2 > \xi_1. \quad (8)$$

With the notations from the main paper, let $\mathbf{A}_\theta^{(r)} = \sum_{k=0}^r \theta_k \mathbf{A}^{[k]}$ denote the θ -weighted variable power operator, where $[\mathbf{A}^{[k]}]_{ij} = \begin{cases} 1 & \text{if } d_{\mathcal{G}}(i, j) = k \\ 0 & \text{o.w.} \end{cases}$ is the k -distance adjacency matrix. Let $\mathbf{A}^{\{k\}}$

denote the nonbacktracking path counting matrix, where the (i, j) -th component indicate the number of self-avoiding paths of graph edges of length k connecting i to j [42]. Our goal is to prove that the top eigenvectors of $\mathbf{A}_\theta^{(r)}$ are asymptotically aligned with those of $\mathbf{A}^{\{k\}}$ for k greater than $\log(n)$ up to a constant multiplicative factor. To do so, we first recall the result of [42], which examines the behaviors of top eigenvectors of $\mathbf{A}^{\{k\}}$.

Lemma 6 ([42]). Assume that (8) holds. Then, w.h.p., for all $k \in \{r/2, \dots, r\}$:

- (a) The operator norm $\|\mathbf{A}^{\{k\}}\|_2$ is up to logarithmic factors $\Theta(\xi_1^k)$. The second eigenvalue of $\mathbf{A}^{\{k\}}$ is up to logarithmic factors $\Omega(\xi_2^k)$.
- (b) The leading eigenvector is asymptotically aligned with $\mathbf{A}^{\{k\}}\mathbf{1}$:

$$\frac{\mathbf{A}^{\{k\}}\mathbf{A}^{\{k\}}\mathbf{1}}{\|\mathbf{A}^{\{k\}}\mathbf{A}^{\{k\}}\mathbf{1}\|_2} = \frac{\mathbf{A}^{\{k\}}\mathbf{1}}{\|\mathbf{A}^{\{k\}}\mathbf{1}\|_2} + \mathbf{h}_k$$

where $\|\mathbf{h}_k\| = o(1)$. The second eigenvector is asymptotically aligned with $\mathbf{A}^{\{k\}}\boldsymbol{\nu}$:

$$\frac{\mathbf{A}^{\{k\}}\mathbf{A}^{\{k\}}\boldsymbol{\nu}}{\|\mathbf{A}^{\{k\}}\mathbf{A}^{\{k\}}\boldsymbol{\nu}\|_2} = \frac{\mathbf{A}^{\{k\}}\boldsymbol{\nu}}{\|\mathbf{A}^{\{k\}}\boldsymbol{\nu}\|_2} + \mathbf{h}'_k$$

where $\|\mathbf{h}'_k\| = o(1)$.

Now, we first define $\Gamma_{\boldsymbol{\theta}}^{\{r\}} = \sum_{k=r/2}^r \theta_k \mathbf{A}^{\{k\}}$, so

$$\mathbf{A}_{\boldsymbol{\theta}}^{(r)} = \Gamma_{\boldsymbol{\theta}}^{\{r\}} + \Delta_{\boldsymbol{\theta}}^{\{r\}} = \Gamma_{\boldsymbol{\theta}}^{\{r\}} + \mathbf{A}_{\boldsymbol{\theta}}^{(r/2-1)} + \sum_{k=r/2}^r \theta_k (\mathbf{A}^{\{k\}} - \mathbf{A}^{\{k\}}).$$

Also, by [42, Theorem 2.3], the local neighborhoods of vertices do not grow fast, and w.h.p., the graph of $\mathbf{A}_{\boldsymbol{\theta}}^{(r/2-1)}$ has maximum degree $O(\xi_1^{r/2}(\log n)^2)$. Let ϕ be the leading eigenvector of $\mathbf{A}_{\boldsymbol{\theta}}^{(r/2-1)}$, and let v be the node where ϕ is maximum (i.e., $\phi(v) \geq \phi(u)$). Without loss of generality, assume that $\phi(v) > 0$. We have a good control over the first eigenvalue λ_1 of $\mathbf{A}_{\boldsymbol{\theta}}^{(r/2-1)}$ as follows:

$$\begin{aligned} \lambda_1 &= \frac{(\mathbf{A}_{\boldsymbol{\theta}}^{(r/2-1)}\phi)(v)}{\phi(v)} = \frac{\sum_{k=0}^{r/2-1} \sum_{\{u:d_{\mathcal{G}}(u,v)=k\}} \theta_k \phi(u)}{\phi(v)} \\ &= \sum_{k=0}^{r/2-1} \theta_k \sum_{\{u:d_{\mathcal{G}}(u,v)=k\}} \frac{\phi(u)}{\phi(v)} \\ &\leq \sum_{k=0}^{r/2-1} |\theta_k| \sum_{\{u:d_{\mathcal{G}}(u,v)=k\}} 1 \\ &\leq \|\boldsymbol{\theta}\|_{\infty} \sum_{\{u:d_{\mathcal{G}}(u,v)\leq r/2-1\}} 1 \\ &= O(\|\boldsymbol{\theta}\|_1 \xi_1^{r/2} (\log n)^2) \end{aligned}$$

Due to [1, Theorem 2], which proves an identical result of Lemma 6 but for $\mathbf{A}^{\{k\}}$, we know that w.h.p., for $r = \epsilon \log(n)$, we can bound the last term by

$$\left\| \sum_{k=r/2}^r \theta_k (\mathbf{A}^{\{k\}} - \mathbf{A}^{\{k\}}) \right\|_2 \leq \sum_{k=0}^r |\theta_k| \|\mathbf{A}^{\{k\}} - \mathbf{A}^{\{k\}}\|_2 = O\left(\|\boldsymbol{\theta}\|_1 \xi_1^{r/2} (\log n)^4\right)$$

Therefore, by triangle inequality, we can conclude that

$$\|\Delta_{\boldsymbol{\theta}}^{\{r\}}\|_2 = \|\mathbf{A}_{\boldsymbol{\theta}}^{(r)} - \Gamma_{\boldsymbol{\theta}}^{\{r\}}\|_2 = O\left(\|\boldsymbol{\theta}\|_1 \xi_1^{r/2} (\log n)^4\right). \quad (9)$$

Now, our goal is to show a similar result as Lemma 6 for $\Gamma_{\boldsymbol{\theta}}^{\{r\}}$. In particular,

$$\frac{\|\Gamma_{\boldsymbol{\theta}}^{\{r\}}\mathbf{A}^{\{r\}}\mathbf{1}\|_2}{\|\mathbf{A}^{\{r\}}\mathbf{1}\|_2} = \left\| \sum_{k=r/2}^r \theta_k \mathbf{A}^{\{k\}} \frac{\mathbf{A}^{\{r\}}\mathbf{1}}{\|\mathbf{A}^{\{r\}}\mathbf{1}\|_2} \right\|_2 \quad (10)$$

$$= \left\| \sum_{k=r/2}^r \theta_k \mathbf{A}^{\{k\}} \frac{\mathbf{A}^{\{k\}}\mathbf{1}}{\|\mathbf{A}^{\{k\}}\mathbf{1}\|_2} \right\|_2 + O\left(\sum_{k=r/2}^r |\theta_k| \|\mathbf{A}^{\{k\}}\|_2 \left\| \frac{\mathbf{A}^{\{r\}}\mathbf{1}}{\|\mathbf{A}^{\{r\}}\mathbf{1}\|_2} - \frac{\mathbf{A}^{\{k\}}\mathbf{1}}{\|\mathbf{A}^{\{k\}}\mathbf{1}\|_2} \right\| \right) \quad (11)$$

$$= \left\| \sum_{k=r/2}^r \theta_k \mathbf{A}^{\{k\}} \frac{\mathbf{A}^{\{k\}} \mathbf{1}}{\|\mathbf{A}^{\{k\}} \mathbf{1}\|_2} \right\|_2 + O \left(\sum_{k=r/2}^r |\theta_k| \xi_1^k n^{-\delta} \right) \quad (12)$$

$$= \left\| \sum_{k=r/2}^r \theta_k \mathbf{A}^{\{k\}} \frac{\mathbf{A}^{\{k\}} \mathbf{1}}{\|\mathbf{A}^{\{k\}} \mathbf{1}\|_2} \right\|_2 + O(\|\boldsymbol{\theta}\|_1 \xi_1^r n^{-\delta}) \quad (13)$$

$$= \left\| \sum_{k=r/2}^r \theta_k \left(\frac{\mathbf{A}^{\{k\}} \mathbf{1}}{\|\mathbf{A}^{\{k\}} \mathbf{1}\|_2} + \mathbf{h}_k \right) \frac{\|\mathbf{A}^{\{k\}} \mathbf{A}^{\{k\}} \mathbf{1}\|_2}{\|\mathbf{A}^{\{k\}} \mathbf{1}\|_2} \right\|_2 + O(\|\boldsymbol{\theta}\|_1 \xi_1^r n^{-\delta}) \quad \text{for } \|\mathbf{h}_k\|_2 = o(1) \quad (14)$$

$$= \left\| \sum_{k=r/2}^r \theta_k \left(\frac{\mathbf{A}^{\{r\}} \mathbf{1}}{\|\mathbf{A}^{\{r\}} \mathbf{1}\|_2} + \mathbf{h}_k \right) \frac{\|\mathbf{A}^{\{k\}} \mathbf{A}^{\{k\}} \mathbf{1}\|_2}{\|\mathbf{A}^{\{k\}} \mathbf{1}\|_2} \right\|_2 + O \left(\left\| \sum_{k=r/2}^r \theta_k \frac{\|\mathbf{A}^{\{k\}} \mathbf{A}^{\{k\}} \mathbf{1}\|_2}{\|\mathbf{A}^{\{k\}} \mathbf{1}\|_2} \right\|_2 \left\| \frac{\mathbf{A}^{\{r\}} \mathbf{1}}{\|\mathbf{A}^{\{r\}} \mathbf{1}\|_2} - \frac{\mathbf{A}^{\{k\}} \mathbf{1}}{\|\mathbf{A}^{\{k\}} \mathbf{1}\|_2} \right\| \right) + O(\|\boldsymbol{\theta}\|_1 \xi_1^r n^{-\delta}) \quad (15)$$

$$= \left\| \sum_{k=r/2}^r \theta_k \left(\frac{\mathbf{A}^{\{r\}} \mathbf{1}}{\|\mathbf{A}^{\{r\}} \mathbf{1}\|_2} + \mathbf{h}_k \right) \frac{\|\mathbf{A}^{\{k\}} \mathbf{A}^{\{k\}} \mathbf{1}\|_2}{\|\mathbf{A}^{\{k\}} \mathbf{1}\|_2} \right\|_2 + O(\|\boldsymbol{\theta}\|_1 \xi_1^r n^{-\delta}) \quad (16)$$

$$= \left(\sum_{k=r/2}^r |\theta_k| \frac{\|\mathbf{A}^{\{k\}} \mathbf{A}^{\{k\}} \mathbf{1}\|_2}{\|\mathbf{A}^{\{k\}} \mathbf{1}\|_2} \right) (1 + o(1)) + O(\|\boldsymbol{\theta}\|_1 \xi_1^r n^{-\delta}) \quad (17)$$

$$= O(\|\boldsymbol{\theta}\|_1 \xi_1^r n^{-\delta}), \quad (18)$$

where (11) and (15) are due to triangle inequalities, (12) and (16) are due to results in [42], and (14) is due to Lemma 6. Therefore, we have $\|\Gamma_{\boldsymbol{\theta}}^{\{r\}} \mathbf{A}^{\{r\}} \mathbf{1}\|_2 = \Theta(\|\boldsymbol{\theta}\|_1 \xi_1^r \|\mathbf{A}^{\{r\}} \mathbf{1}\|_2)$. Similarly, we can prove that $\|\Gamma_{\boldsymbol{\theta}}^{\{r\}} \mathbf{A}^{\{r\}} \boldsymbol{\nu}\|_2 = \Theta(\|\boldsymbol{\theta}\|_1 \xi_2^r \|\mathbf{A}^{\{r\}} \boldsymbol{\nu}\|_2)$.

Furthermore, we can show that $\Gamma_{\boldsymbol{\theta}}^{\{r\}}$ satisfies the weak Ramanujan property (the proof is similar to [42] and is deferred to Section D).

Lemma 7. For any fixed $\epsilon > 0$, $\Gamma_{\boldsymbol{\theta}}^{\{r\}}$ satisfies the following weak Ramanujan property w.h.p.,

$$\sup_{\|\mathbf{u}\|_2=1, \mathbf{u}^\top \mathbf{A}^{\{r\}} \mathbf{1} = \mathbf{u}^\top \mathbf{A}^{\{r\}} \boldsymbol{\nu} = 0} \|\Gamma_{\boldsymbol{\theta}}^{\{r\}} \mathbf{u}\|_2 = \|\boldsymbol{\theta}\|_1 n^{\epsilon} \xi_1^{r/2} O(\log(n))$$

By Lemma 7, the leading two eigenvectors of $\Gamma_{\boldsymbol{\theta}}^{\{r\}}$ will be asymptotically in the span of $\mathbf{A}^{\{r\}} \mathbf{1}$ and $\mathbf{A}^{\{r\}} \boldsymbol{\nu}$ according to the variational definition of eigenvalues. By our previous analysis, this means that the top eigenvalue of $\Gamma_{\boldsymbol{\theta}}^{\{r\}}$ will be $\Theta(\|\boldsymbol{\theta}\|_1 \xi_1^r)$ with eigenvector asymptotically aligned with $\mathbf{A}^{\{r\}} \mathbf{1}$. Since by [42, Lemma 4.4], $\mathbf{A}^{\{r\}} \mathbf{1}$ and $\mathbf{A}^{\{r\}} \boldsymbol{\nu}$ are asymptotically orthogonal, the second eigenvalue of $\Gamma_{\boldsymbol{\theta}}^{\{r\}}$ will be $\Theta(\|\boldsymbol{\theta}\|_1 \xi_2^r)$ with eigenvector asymptotically aligned with $\mathbf{A}^{\{r\}} \boldsymbol{\nu}$.

Since the perturbation term $\|\Delta_{\boldsymbol{\theta}}^{\{r\}}\|_2 = o(\lambda_2(\Gamma_{\boldsymbol{\theta}}^{\{r\}}))$ by (9), using Weyl's inequality [52], we can conclude that the leading eigenvalue $\lambda_1(\mathbf{A}_{\boldsymbol{\theta}}^{(r)}) = \Theta(\|\boldsymbol{\theta}\|_1 \xi_1^r)$, the second eigenvalue $\lambda_2(\mathbf{A}_{\boldsymbol{\theta}}^{(r)}) = \Theta(\|\boldsymbol{\theta}\|_1 \xi_2^r)$, and the rest of the eigenvalues are bounded by $\|\boldsymbol{\theta}\|_1 n^{\epsilon} \xi_1^{r/2} O(\log(n))$. Moreover, since $\|\Delta_{\boldsymbol{\theta}}^{\{r\}}\|_2 = o(\max\{\lambda_1(\Gamma_{\boldsymbol{\theta}}^{\{r\}}) - \lambda_2(\Gamma_{\boldsymbol{\theta}}^{\{r\}}), \lambda_2(\Gamma_{\boldsymbol{\theta}}^{\{r\}}) - \lambda_3(\Gamma_{\boldsymbol{\theta}}^{\{r\}})\})$, by the Davis-Kahan Theorem [17], the leading two eigenvectors of $\mathbf{A}_{\boldsymbol{\theta}}^{(r)}$ are asymptotically aligned with $\mathbf{A}^{\{r\}} \mathbf{1}$ and $\mathbf{A}^{\{r\}} \boldsymbol{\nu}$, which is shown to be enough for the rounding procedure of [42] to achieve weak recovery.

D Proof of Lemma 7

Denote $\tilde{\mathbf{A}} = \frac{a_{\text{intra}}}{n} [\frac{1}{2}(\mathbf{1}\mathbf{1}^\top + \boldsymbol{\nu}\boldsymbol{\nu}^\top) - \mathbf{I}] + \frac{a_{\text{inter}}}{2n}(\mathbf{1}\mathbf{1}^\top - \boldsymbol{\nu}\boldsymbol{\nu}^\top)$ as the expected adjacency matrix conditioned on community labels $\boldsymbol{\nu}$. Let P_{ij} denote the set of all self-avoiding paths $i_0^k := \{i_0, \dots, i_k\}$ from i to j , such that no nodes appear twice in the path, and define $\mathbf{Q}_{ij}^{\{m\}} := \sum_{i_0^m \in P_{ij}} \prod_{t=1}^m (\mathbf{A} - \tilde{\mathbf{A}})_{i_{t-1}i_t}$. Let T_{ij}^m be the concatenation of self-avoiding paths i_0^{k-m} and i_{k-m+1}^k , and let R_{ij}^m denote $T_{ij}^m \setminus P_{ij}$. Define $\mathbf{W}_{ij}^{\{k,m\}} := \sum_{i_0^k \in R_{ij}^m} \prod_{t=1}^{k-m} (\mathbf{A} - \tilde{\mathbf{A}})_{i_{t-1}i_t} \tilde{\mathbf{A}}_{i_{k-m}i_{k-m+1}} \prod_{t=k-m+2}^k (\mathbf{A})_{i_{t-1}i_t}$. Then, by [42, Theorem 2.2], we can have

$$\mathbf{A}^{\{k\}} = \mathbf{Q}^{\{k\}} + \sum_{m=1}^k (\mathbf{Q}^{\{k-m\}} \tilde{\mathbf{A}} \mathbf{A}^{\{m-1\}}) - \sum_{m=1}^k \mathbf{W}^{\{k,m\}}.$$

Hence,

$$\begin{aligned} \boldsymbol{\Gamma}_\theta^{\{r\}} &= \sum_{k=r/2}^r \theta_k \mathbf{A}^{\{k\}} \\ &= \sum_{k=r/2}^r \theta_k \mathbf{Q}^{\{k\}} + \sum_{k=r/2}^r \theta_k \sum_{m=1}^k (\mathbf{Q}^{\{k-m\}} \tilde{\mathbf{A}} \mathbf{A}^{\{m-1\}}) - \sum_{k=r/2}^r \sum_{m=1}^k \theta_k \mathbf{W}^{\{k,m\}} \\ &= \sum_{k=r/2}^r \theta_k \mathbf{Q}^{\{k\}} + \sum_{m=1}^r \left(\sum_{k=\max(r/2, m)}^r \theta_k \mathbf{Q}^{\{k-m\}} \tilde{\mathbf{A}} \right) \mathbf{A}^{\{m-1\}} - \sum_{k=r/2}^r \sum_{m=1}^k \theta_k \mathbf{W}^{\{k,m\}}. \end{aligned}$$

In particular, for any \mathbf{u} that is orthogonal to $\mathbf{A}^{\{m\}} \mathbf{1}$ and $\mathbf{A}^{\{m\}} \boldsymbol{\nu}$ with norm-1 (i.e., a feasible vector of the variational definition in Lemma 7), we have:

$$\begin{aligned} \|\boldsymbol{\Gamma}_\theta^{\{r\}} \mathbf{u}\|_2 &\leq \rho \left(\sum_{k=r/2}^r \theta_k \mathbf{Q}^{\{k\}} \right) + \sum_{m=1}^r \sum_{k=\max(r/2, m)}^r |\theta_k| \rho(\mathbf{Q}^{\{k-m\}}) \|\tilde{\mathbf{A}} \mathbf{A}^{\{m-1\}} \mathbf{u}\|_2 \\ &\quad + \rho \left(\sum_{k=r/2}^r \theta_k \sum_{m=1}^k \mathbf{W}^{\{k,m\}} \right) \end{aligned}$$

Since by [42], the terms $\rho(\mathbf{Q}^{\{k\}})$ and $\rho(\mathbf{W}^{\{k,m\}})$ are bounded by $n^\epsilon \xi_1^{r/2}$, $\|\tilde{\mathbf{A}} \mathbf{A}^{\{m-1\}} \mathbf{x}\|_2$ is bounded by $O(\log(n) + \sqrt{\log(n) \xi_1^{m-1}})$, with some elementary calculations, we have that $\|\boldsymbol{\Gamma}_\theta^{\{r\}} \mathbf{u}\|_2$ is bounded by $\|\boldsymbol{\theta}\|_1 n^\epsilon \xi_1^{r/2} O(\log(n))$.

E More experimental results

Visualization of network embeddings. We used t-SNE [40] to visualize the network embeddings learned by r-GCN (Figure 6) and VPN (Figure 7) for Citeseer, Cora and Pubmed. As can be seen, with very limited labels, the proposed methods can learn an effective embedding of the nodes.

Evasion experiment. We provide the post-evasion accuracy for Citeseer, Cora, and Pubmed in Table 3. Results are obtained with 20 random initializations on a given attacked network.

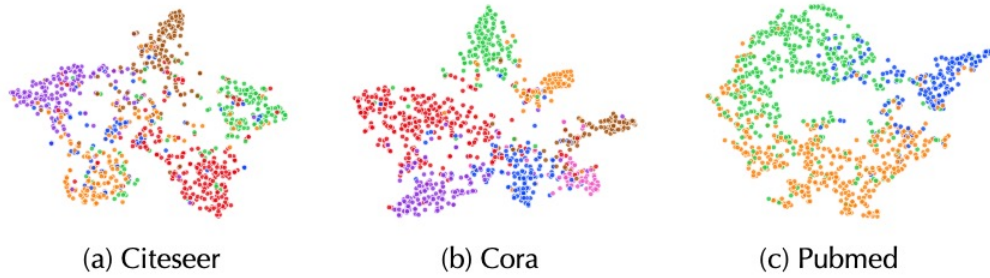


Figure 6: t-SNE visualization of network embeddings learned by r-GCN.

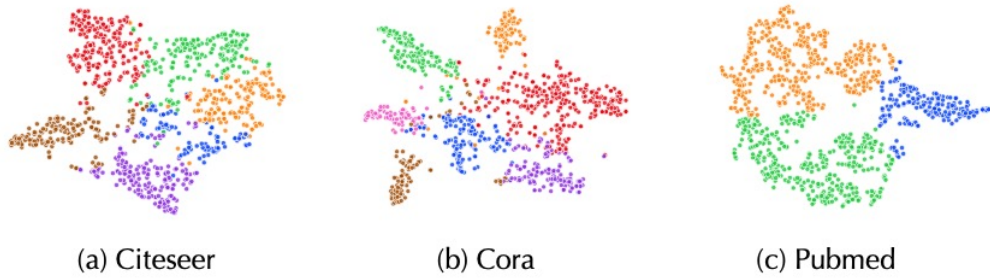


Figure 7: t-SNE visualization of network embeddings learned by VPN.

Table 3: Summary of evasion attack performance in terms of post-attack accuracy (in percent).

		Attack rate (% edge)					
		5	10	15	20	25	30
Citeseer	GCN	68.5	66.3	63.4	62.8	60.8	57.5
	r-GCN	70.1	68.9	67.6	66.0	64.5	62.7
	VPN	69.5	68.2	66.5	65.1	63.8	61.1
Cora	GCN	79.2	76.7	74.3	72.5	70.2	69.9
	r-GCN	79.3	77.0	74.6	73.3	71.6	72.5
	VPN	79.2	76.9	74.8	73.1	71.3	71.9
Pubmed	GCN	75.3	73.0	71.6	69.2	68.1	67.1
	r-GCN	76.5	74.7	71.9	69.8	68.1	67.2
	VPN	76.0	73.7	71.7	69.5	68.3	67.1